Available online at www.sciencedirect.com
ScienceDirect
Progress in Natural Science 19 (2009) 1119–1124
Progress in Natural Science
www.elsevier.com/locate/pnsc

Research into a theoretical mode of coherent structures in the wall region of a turbulent boundary layer induced by a wall local disturbance

Changgen Lu [a,*], Qinjuan Qi [b]

[a] College of Atmospheric Sciences, Nanjing University of Information Science & Technology, Nanjing 210044, China
[b] College of Public Management, Nanjing University of Information Science & Technology, Nanjing 210044, China

Received 17 September 2008; received in revised form 6 October 2008; accepted 7 October 2008

Abstract

The idea of applying direct numerical simulation (DNS), a theoretical mode of coherent structures in the wall region of a turbulent boundary layer, has been discussed in the literature. The various aspects of the formation mechanism of the coherent structures agree well with both DNS and experimental results. In addition, a close relationship has been found between the evolutional characteristics and factors such as the magnitude and structural distribution of the wall local impulse disturbance, and the amount of energy a local disturbance introduces into the wall region. Moreover, these parameters play key roles in the formation of coherent structures near the wall region of a turbulent boundary layer. Therefore, the wall local impulse disturbance provides a theoretical model for triggering the formation of coherent structures in the wall region of a turbulent boundary layer.

Keywords: Turbulent boundary layer; Wall region; Coherent structure; Local disturbance

1. Introduction

Since turbulence is universal in nature, understanding its behaviour is central to the theory of hydrodynamics and for being able to solve practical engineering problems. In the 1960s, Kline et al. [1] discovered flow structures (e.g. slow-speed streaks, high-speed streaks and bursts), overthrowing the commonly held belief that turbulence is a totally anomalous and stochastic motion. In recent times, there has been much interest in the formation mechanism and nonlinear evolutional characteristics of the coherent structures in the wall region of a turbulent boundary layer. Many recent investigations into direct numerical simulation (DNS) have shown that there is significant commonality between many aspects of the coherent structures in the wall region of a turbulent boundary layer and those of unstable waves in laminar boundary layer transition. As a result, the coherent structures of turbulence can be described using an unstable wave of hydrodynamic stability. Jang et al. [2] applied a quasi-laminar model and direct resonance theory to calculate the selective wave numbers of a disturbance wave and came to the conclusion that the spacing between streaks is about 90 viscous units. In Ref. [3], some significant results were found by making use of resonance three-wave theory to study numerically the origin and nature of the coherent structures in the wall region of a turbulent boundary layer. In Ref. [4], a period of resonance three-wave model was applied numerically as a theoretical model of individual coherent structures in order to study its evolution. It was found that some characteristics are consistent with experimental observation. However,

* Corresponding author. Tel.: +86 25 86204028; fax: +86 25 58699941.
E-mail address: lu678q@163.com (C. Lu).

1002-0071/$ - see front matter © 2009 National Natural Science Foundation of China and Chinese Academy of Sciences. Published by Elsevier Limited and Science in China Press. All rights reserved.
doi:10.1016/j.pnsc.2008.10.011

all these theoretical investigations used hydrodynamic stability theory to describe the nature of unstable waves so that it was not possible to identify the exact locations of their origins, let alone a perfect model of the interrelated structure. In order to overcome this limitation, some studies were carried out on the formation mechanism of the coherent structures induced by the local disturbance on the outskirt of the wall region of a turbulent boundary layer [5]. Although there is some argument for this approach, it does not completely explain the reason for the appearance of outskirt disturbances. Thus, its contribution is limited to a physical mechanism for explaining the formation of the coherent structure. Taking all these into account, together with the observations of the phenomenon revealed in Reynolds's experiment that some small local disturbances on the wall of a pipe can accelerate the instability of the flow in the transition of flow from laminar to turbulent, we may conclude that local disturbances which existed on the wall can also produce coherent structures. However, it does not help to reveal the underlying inducing mechanisms. The extent of our understanding of this will determine the quality of the theoretical model of the coherent structures in the wall region of a turbulent layer. It is necessary to understand turbulent formation and the transmission of momentum and energy of the turbulence in this process so that ultimately an accurate model of turbulence can be established.

2. Basic equations and numerical methods

The basic equations are the Navier–Stokes (N–S) equation and the continuity equation:

$$\partial \boldsymbol{u}/\partial t + (\boldsymbol{u}\cdot\nabla)\boldsymbol{u} = -\nabla p + (1/Re)\nabla^2\boldsymbol{u} \quad (1)$$

$$\nabla\cdot\boldsymbol{u} = 0 \quad (2)$$

where $\boldsymbol{u}$ is the velocity, p the pressure, Re the Reynolds number, ∇ the gradient operator, and ∇^2 the Laplace operator.

For our purpose, the velocity and pressure are decomposed as follows: $\boldsymbol{u} = \boldsymbol{U} + \boldsymbol{u}'$; $p = P + p'$, where $\boldsymbol{U}$ is a complex velocity of the basic flow, $\boldsymbol{u}'$ is the disturbance velocity of the coherent structure, P the pressure of the basic flow, and p' the disturbance pressure of the coherent structure. If the basic flow is known, the solution can be obtained by solving the N–S equation. This is presented in Ref. [4] in detail and therefore not repeated here. Since the region of interest is the region very close to the wall (limited to 100 viscous lengths from the wall), the small-scale turbulence there is very weak. This assertion is supported by several arguments, but the most direct evidence can be found in a figure of Ref. [6], obtained by direct numerical simulation, in which the velocity field in a normal cross-section at the location where a coherent structure existed was shown. Apart from the large eddies of the size of coherent structures, there is no obvious small-scale motion. Therefore, the quasi-laminar-flow assumption is adopted in this paper. The numerical method for solving Eq. (1) is shown in detail in Ref. [7].

3. Calculation region and boundary condition

The calculation region is defined as follows:

The streamwise: $0 \leqslant x \leqslant 33$; the vertical: $0 \leqslant y \leqslant 0.88$; the spanwise: $-6 \leqslant z \leqslant 6$.

The calculation grids: $\{x, y, z\} = \{200, 200, 32\}$.

Inlet boundary condition: $x = 0$, $u' = 0$, $p' = 0$

Outlet boundary condition:

$$x = 33, \quad \boldsymbol{u}' = 0, \quad \partial p'/\partial x = 0$$

Boundary condition at the upper boundary:

$$y = 0.88, \quad \partial \boldsymbol{u}'/\partial y + \alpha \boldsymbol{u}' = 0, \quad \partial p/\partial y = 0$$

The boundary condition at the wall boundary: $y = 0$, the non-dimensional initial impulsive time $t \leqslant 10$, and $v = A_0 \sin[\pi(x - 2.6)/1.3] \cos[\pi z/3]$, which are distributed in the streamwise grid ($1.33 < x < 4.0$), and in the spanwise grid ($-1.5 < z < 1.5$) where A_0 is the initial amplitude of the local disturbance, and the rest of the grids are $\boldsymbol{u}' = 0$, $\partial p'/\partial x = 0$. The impulse at the wall is removed when $t > 10$, and all the grids are $\boldsymbol{u}' = 0$. Fig. 1(a) shows the symmetrical structure. The magnitude and distribution of the nonsymmetrical structure is identical to that of the symmetrical case; only the symmetrical structure is shifted by 60° to the x-axis. Fig. 1(b) shows the corresponding nonsymmetrical structure.

The Reynolds number, Re, in this case, equals 50,000. In this case, Re represents $U_0\delta/v$, where U_0 is the free streamwise velocity, δ the nominal thickness of the Blasius profile

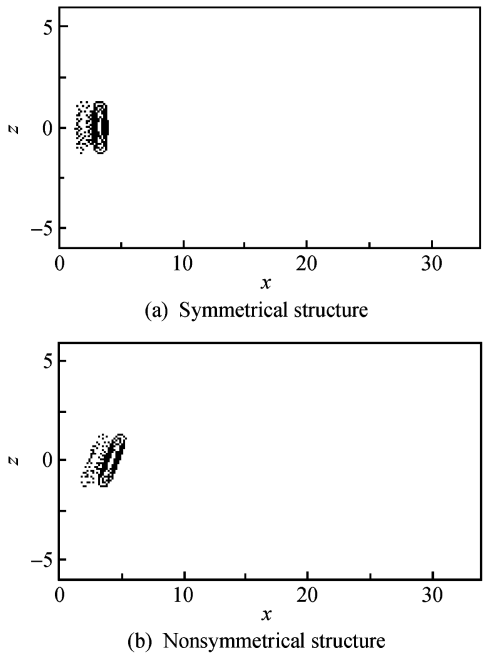

(a) Symmetrical structure

(b) Nonsymmetrical structure

Fig. 1. Contour distribution of the initial local disturbance velocity in the normal direction.

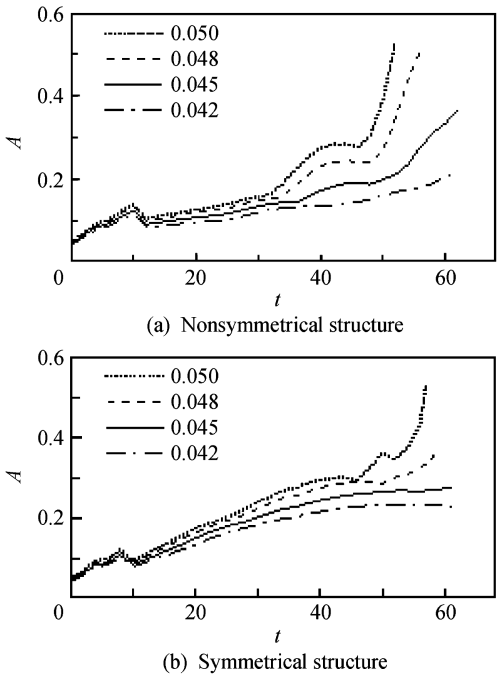

Fig. 2. The evolution of the amplitudes.

which is compressed in the y direction such that a part of it can join smoothly the turbulent flow profile ($y^+ = 100$) at the inflow location. The time step (Δt) equals 0.02. The initial value of the disturbing velocity $\boldsymbol{u}'$ is 0.

4. Results and analyses

For all the cases, we assume that the initial amplitudes (A_0) are 0.050, 0.048, 0.045, and 0.042. The amplitude of the coherent structures, A, is given by:

$$A = \sqrt{|u|^2_{\max} + |v|^2_{\max} + |w|^2_{\max}} \tag{3}$$

We have proved that the coherent structures in the wall region of a turbulent boundary layer induced by the wall initial local disturbance can exist as a symmetrical or nonsymmetrical structure in the z direction. But the latter can be triggered and grow far more easily. Then, the evolution of the amplitudes for the cases is shown in Fig. 2, from which an initial increase in amplitudes can be seen, followed by a transient decline when $t \geqslant 10$, and then, recovery but a very slow growth before a final jump. Throughout the evolution, the growth rates of both the symmetrical and nonsymmetrical coherent structures in the wall region of a turbulent boundary layer show an accelerative tendency. In the case of symmetrical coherent structures, initially, it is always slightly larger than that of the nonsymmetrical one. However, after a certain degree of evolution, it remains far below the level of its counterpart induced by wall initial local disturbances.

Fig. 3 shows the velocity projection on the three planes normal to the streamwise direction for a faster growing case ($A_0 = 0.048$). The first plane is at the location where the spanwise velocity takes its maximum value, from which we can clearly see its nonsymmetrical and symmetrical streamwise eddies. As time goes by, the structural intensity of the streamwise eddies strengthens and the center of the streamwise eddies rise up gradually. However, the strength of the nonsymmetrical streamwise eddies is much higher than that of the symmetrical ones. Fig. 3 shows that the evolution of the symmetrical and nonsymmetrical streamwise eddies we observed are similar to those of the modeling of individual coherent structures in the wall region of the turbulent boundary layers in Ref. [4].

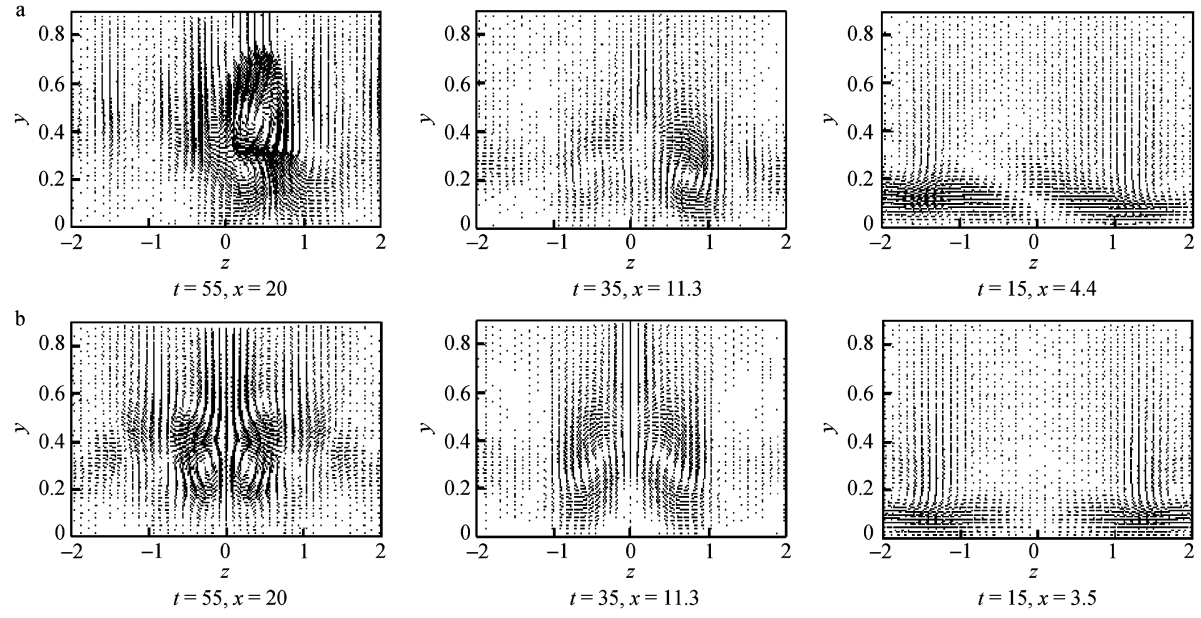

Fig. 3. Nonsymmetrical streamwise eddies (a) and symmetrical streamwise eddies (b) in the y–z plane.

Fig. 4 shows the variation in the spanwise velocity profiles at the maximal location at different times ($A_0 = 0.048$). As shown in Fig. 4, the differences are very small in magnitude, position and distribution of the maximal spanwise velocity at the same time at the beginning stage between the symmetrical and nonsymmetrical coherent structures. However, during the subsequent nonlinear evolution, the effect of the nonsymmetrical coherent structures gradually becomes obvious. When $t = 55$, the absolute value of the maximal spanwise velocity of the nonsymmetrical coherent structures surpasses that of the symmetrical ones at the large scale. At the moment, there is a significant difference between their distribution of spanwise velocity profiles, that is, the three-dimensional characteristics of the nonsymmetrical coherent structures are greatly strengthened, which favors the rapid formation and development of structures of streamwise eddies, accelerating the production of "bursting".

Fig. 5 shows the variation in the mean velocity profiles at $t = 15$, 35, and 55, where the complex velocity profile and the velocity profile of the low- and high-speed streaks are represented by broken lines, real lines and dotted lines, respectively. Fig. 6 shows the contour distribution of the maximal streamwise disturbance velocity at different times ($A_0 = 0.048$), with intervals of about 0.02. Under the effect of a nonsymmetrical local disturbance, the coherent structure in the wall region of the turbulent boundary layer appears and moves downstream. The structure of the high-speed streaks and that of the low-speed streaks stagger each other and are completely nonsymmetrical. Specifically, they gradually strengthen as time goes by. In essence, throughout the process, the incidence of the individual coherent structure is totally limited to a certain local area, and powerful shear layers in some local positions are formed. Moreover, the flow begins to become unstable. Thus, an inflexion point and twisting may appear in the mean velocity profile, leading to strong oscillations and a big impulse, namely "bursting".

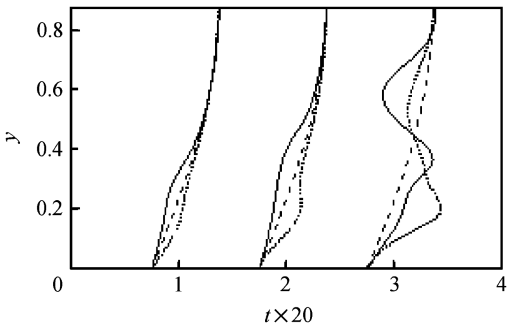

Fig. 5. Change in the mean velocity profile over time.

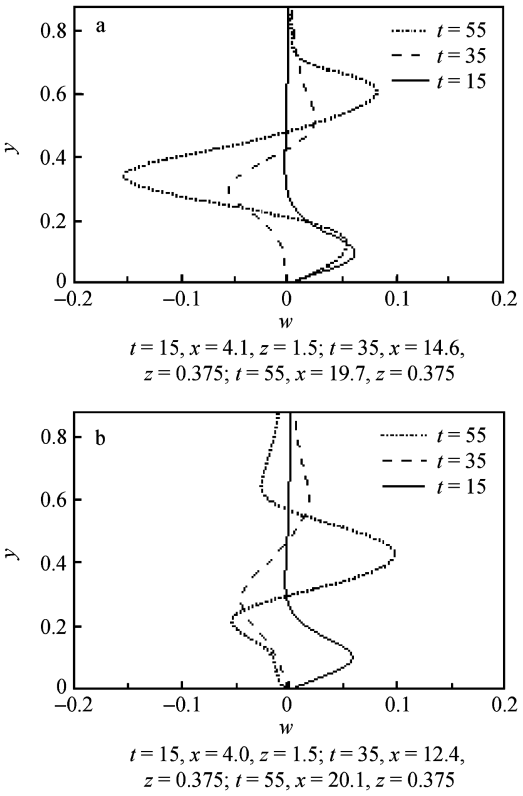

Fig. 4. Spanwise velocity with y at the maximal location: (a) nonsymmetrical structure and (b) symmetrical structure.

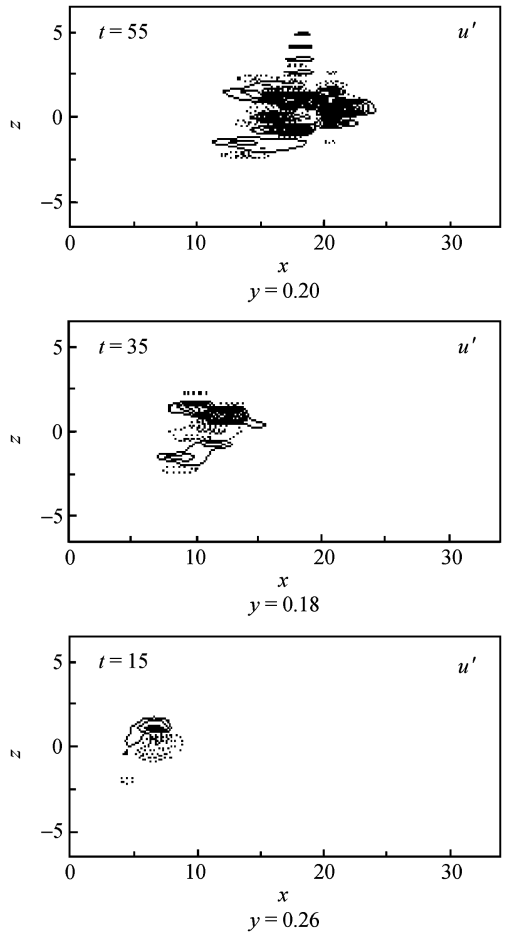

Fig. 6. Iso-contour for u' in a plane for $t = 15$, 35, and 55. Solid line $u' > 0$; broken line $u' < 0$.

We can also calculate the propagation speed of the coherent structures. As the shape of the coherent structure does not remain constant, we cannot define a clear out propagation speed. However, we can focus on the position where the positive or negative u' component of the disturbance speed takes on its maximum value. Then, from the distance, it travels during a fixed time period, we can calculate its mean speed, and the mean of the positive and negative u' component of the disturbance speed can be seen as the propagation speed of the structure. We have calculated the propagation speed for all coherent structures, and the average speed of propagation is found to be $9.9u^+$, where u^+ is the friction velocity. Compared with the value $10.0u^+$, which is estimated from DNS for a turbulent channel flow, the result is satisfactory.

Fig. 7 shows the evolution of the amplitudes for different features and the energy of the coherent structures in the wall region of a turbulent boundary layer induced by the wall local initial disturbance ($A_0 = 0.048$), where curves 1 and 2 in the figure represent the evolution of the amplitudes of the symmetrical and nonsymmetrical coherent structures. In addition, curves 3, 4, and 5 represent those of the coherent structures in the wall region of a turbulent boundary layer induced by the wall local initial nonsymmetrical even rhombic distribution disturbance, whose energy equals 1.0, 0.7, and 0.54 times the energy of the wall local initial nonsymmetrical disturbance, respectively. It is clear that the coherent structure in the wall region of a turbulent boundary layer, which is induced by the larger energy of the wall local initial disturbance, is formed rather more easily. In contrast, when the energy of the wall local initial disturbance, which is introduced into the wall region, is less, it becomes more difficult (and sometimes impossible) to trigger the production of coherent structures in the wall region of a turbulent boundary layer. Although the wall local initial disturbance energy is identical, the growth rate of the coherent structure can be different, due to the different structure or distribution of the wall local initial disturbance. The coherent structures in the wall region of a turbulent boundary layer were induced by the nonsymmetrical, even rhombic, initial wall local disturbance trigger comparatively easily. This is followed by the nonsymmetrical initial wall local disturbances in the structures and the symmetrical ones. As a result, the formation mechanism of the coherent structure in the wall region lies in the initial disturbance energy, the nature of the characteristic, the initial disturbance structure and the distribution.

Fig. 8 shows the Reynolds stress profiles ($A_0 = 0.048$), where the representations of curves 1, 2, 3, 4, and 5 are the same as those in Fig. 7. As time goes on, the nonlinear reaction of the coherent structures become stronger and stronger, triggering the rapid growth in the Reynolds stress of the coherent structures in the wall region. As shown in Fig. 8, the more initial energy introduced into the near-wall region, the more drastic the change in the Reynolds stress. In contrast, when the initial energy, which is introduced into the near-wall region of a turbulent boundary layer, is less than a certain threshold, there will not be any coherent structures formed in the wall region of a turbulent boundary layer. Therefore, the Reynolds stress will increase slowly or tend to attenuate.

In Fig. 9, three groups of curves, namely $a1$ and $a2$, $b1$ and $b2$, $c1$ and $c2$, demonstrate the evolution law of the amplitudes of the coherent structures in the wall region of a turbulent boundary layer, with the former of each set induced by a nonsymmetrical local disturbance and the latter by a symmetrical one, when the loading initial time stands at 15, 10, and 5, respectively ($A_0 = 0.048$).

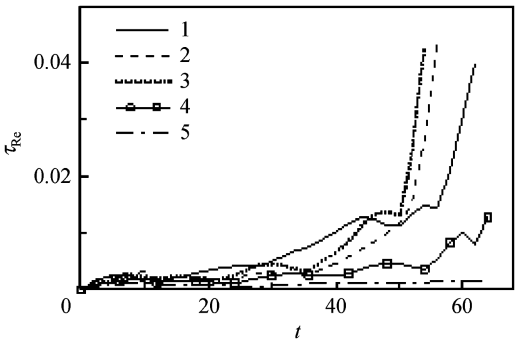

Fig. 8. Maximum in the Reynolds stress over time.

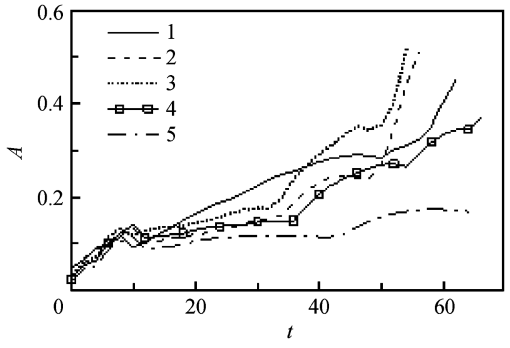

Fig. 7. Under different conditions, the evolution of the amplitudes.

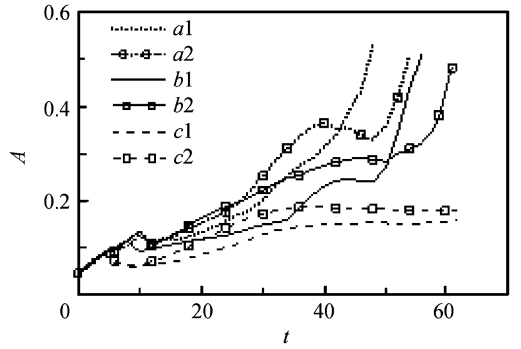

Fig. 9. The evolution of the amplitudes under loading times of the different initial local disturbance.

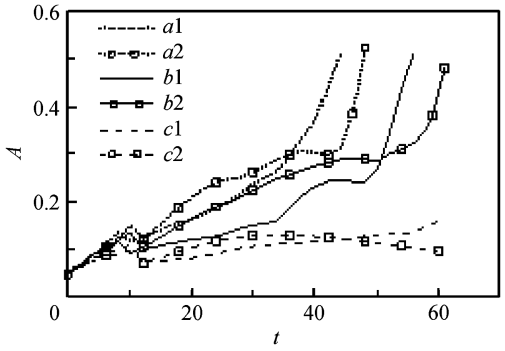

Fig. 10. The evolution of amplitudes under the influence area of different initial local disturbances.

When the loading time of the initial local disturbance goes up, the growth rate of the amplitudes increases gradually. Under the loading time of the same local initial disturbance, the nonsymmetrical cases are always triggered more easily than the symmetrical ones. When the loading time of the local initial disturbance is decreased to a certain threshold, the symmetrical and nonsymmetrical coherent structures in the wall region of a turbulent boundary layer cannot be induced to increase, but tend to attenuate because of the decrease in the loading time of the local initial disturbance and the initial energy introduced into the near-wall region of a turbulent boundary layer.

Considering the change in the disturbing area in the x direction alone, three groups of curves in Fig. 10, namely $a1$ and $a2$, $b1$ and $b2$ and $c1$ and $c2$, illustrate the evolution of the amplitudes of the coherent structures in the wall region of a turbulent boundary layer, with the former of each set induced by the nonsymmetrical local disturbing area and the latter by the symmetrical one, when the corresponding disturbing areas of each are $1.15A$, A and $0.5A$, respectively ($A_0 = 0.048$). While the local initial disturbing area increases gradually, in most cases, the coherent structures in the wall region of a turbulent boundary layer will increase rapidly, and also the nonsymmetrical structures are always triggered more easily than the symmetrical ones. If the initial local disturbing area is relatively smaller, the ability to trigger the coherent structures in the wall region is comparatively weaker and may result in no excitation or formation at all. Generally speaking, in order to inspire the coherent structures in the wall region, the area affected by the initial local disturbance should be sufficiently large to insure that the energy introduced into the near-wall region is sufficient to trigger the coherent structure; otherwise the coherent structures in the wall region will not be able to form.

5. Conclusions

The numerical results have shown that a local disturbance at a certain location is able to trigger nonsymmetrical and symmetrical coherent structures in the wall region of a turbulent boundary layer. It appears that there are many plausible kinds of theoretical models to explain the formation mechanism of the coherent structures in the wall region of a turbulent boundary layer. One such model is presented here. The magnitude of the initial disturbing amplitude, of the loading time, of the influencing area, of the energy introduced into the wall region of a turbulent boundary layer, and the distributing formation of the initial local disturbance are vital for revealing the origin and nature of the coherent structures in the wall region of a turbulent boundary layer. Therefore, the coherent structures are localized and have vertical features. In addition, the propagation speed is close to that found in DNS. This provides evidence to suggest that the model is reasonably good. Therefore, the research presented in this paper on the triggering mechanism for coherent structures in the wall region of a turbulent boundary layer provides a relatively integrated insight into the mechanism involved in the production and maintenance of turbulence in the wall region.

Acknowledgements

This work was supported by the National Natural Science Foundation of China (Grant No. 10672052), the Natural Science Foundation of the Jiangsu Province of China (Grant No. BK2007178), and the Science Foundation of Nanjing University of Information Science & Technology (20080101).

References

[1] Kline SL, Reynolds WC, Schraub FH, et al. The structure of turbulent boundary layers. J Fluid Mech 1967;30:741–74.
[2] Jang PS, Benney DJ, Granl RL. On the region of streamwise vortices in a turbulent boundary layer. J Fluid Mech 1986;169:109–31.
[3] Zhou H, Xiong ZM. The mechanism for the generation of coherent structures in the wall region of a turbulent boundary layer. Sci Chin (Ser A) 1995;38(2):188–94.
[4] Zhou H, Lu CG, Luo JS. Modeling of individual coherent structures in wall region of a turbulent boundary layer. Sci Chin (Ser A) 1999;42(2):627–35.
[5] Zhang DM, Luo JS, Zhou H. A mechanism for the excitation of coherent structures in wall region of a turbulent boundary layer. Appl Math Mech 2005;26(4):379–85.
[6] Gurzennec YG, Piomelli U, Kim J. On the shape and dynamics of wall structures in turbulent channel flow. Phys Fluids 1989;1(4):764–6.
[7] Lu CG, Cao WD, Qian JH. A study on numerical method of Navier–Stokes equations and nonlinear-evolution of the coherent structure in a laminar boundary layer. J Hydrodyn (Ser B) 2006;18(3):110–6.